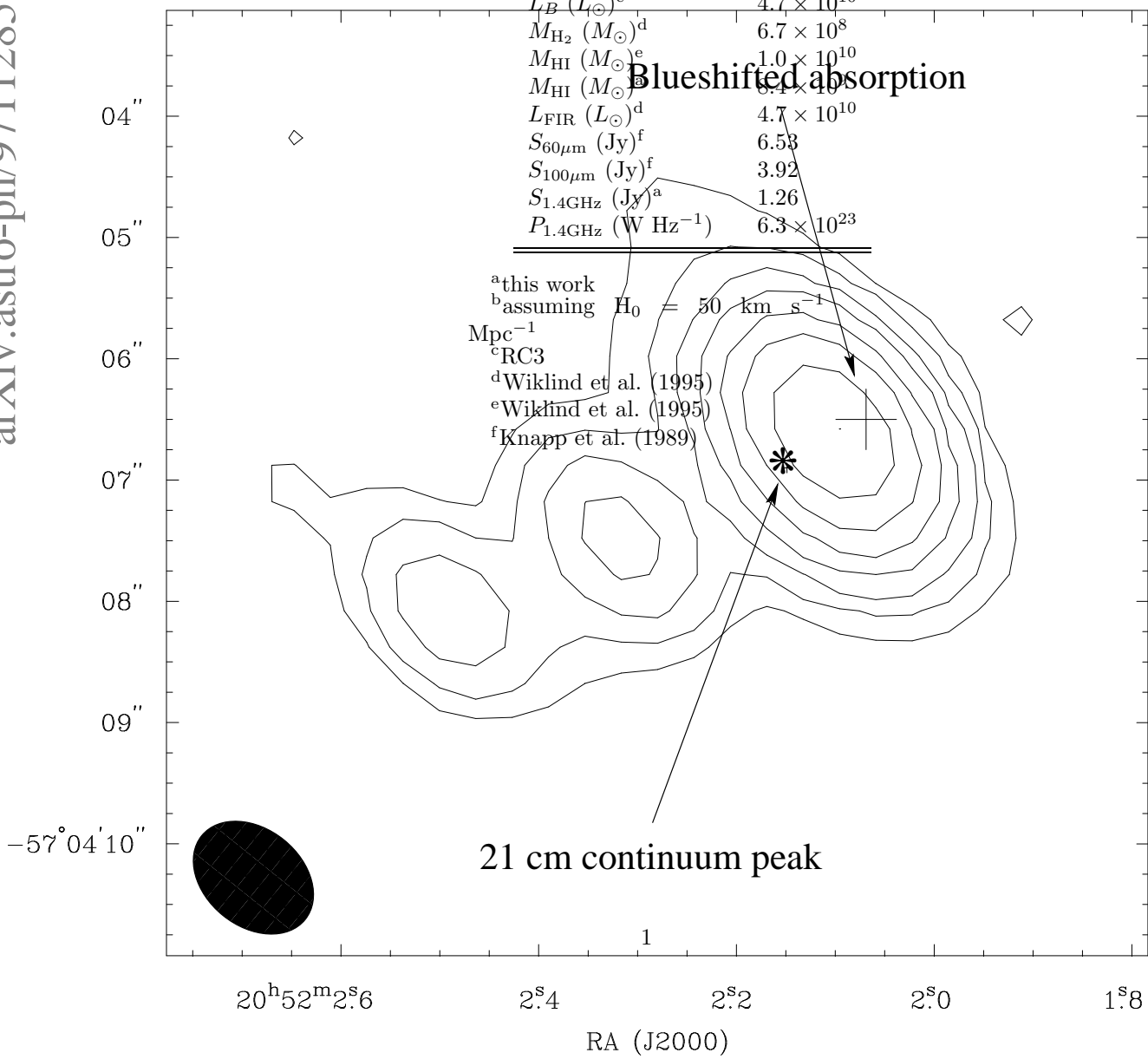


TABLE 1. Properties of IC 5063

v_{helio} (km s ⁻¹) ^a	3404
Distance (Mpc) ^b	68
scale (kpc arcsec ⁻¹)	0.32
L_B (L_{\odot}) ^c	4.7×10^{10}
M_{H_2} (M_{\odot}) ^d	6.7×10^8
M_{HI} (M_{\odot}) ^e	1.0×10^{10}
M_{HI} (M_{\odot}) ^f	8.4×10^9
L_{FIR} (L_{\odot}) ^d	4.7×10^{10}
$S_{60\mu\text{m}}$ (Jy) ^f	6.53
$S_{100\mu\text{m}}$ (Jy) ^f	3.92
$S_{1.4\text{GHz}}$ (Jy) ^a	1.26
$P_{1.4\text{GHz}}$ (W Hz ⁻¹)	6.3×10^{23}

^athis work
^bassuming $H_0 = 50 \text{ km s}^{-1} \text{ Mpc}^{-1}$
^cRC3
^dWiklind et al. (1995)
^eWiklind et al. (1995)
^fKnapp et al. (1989)



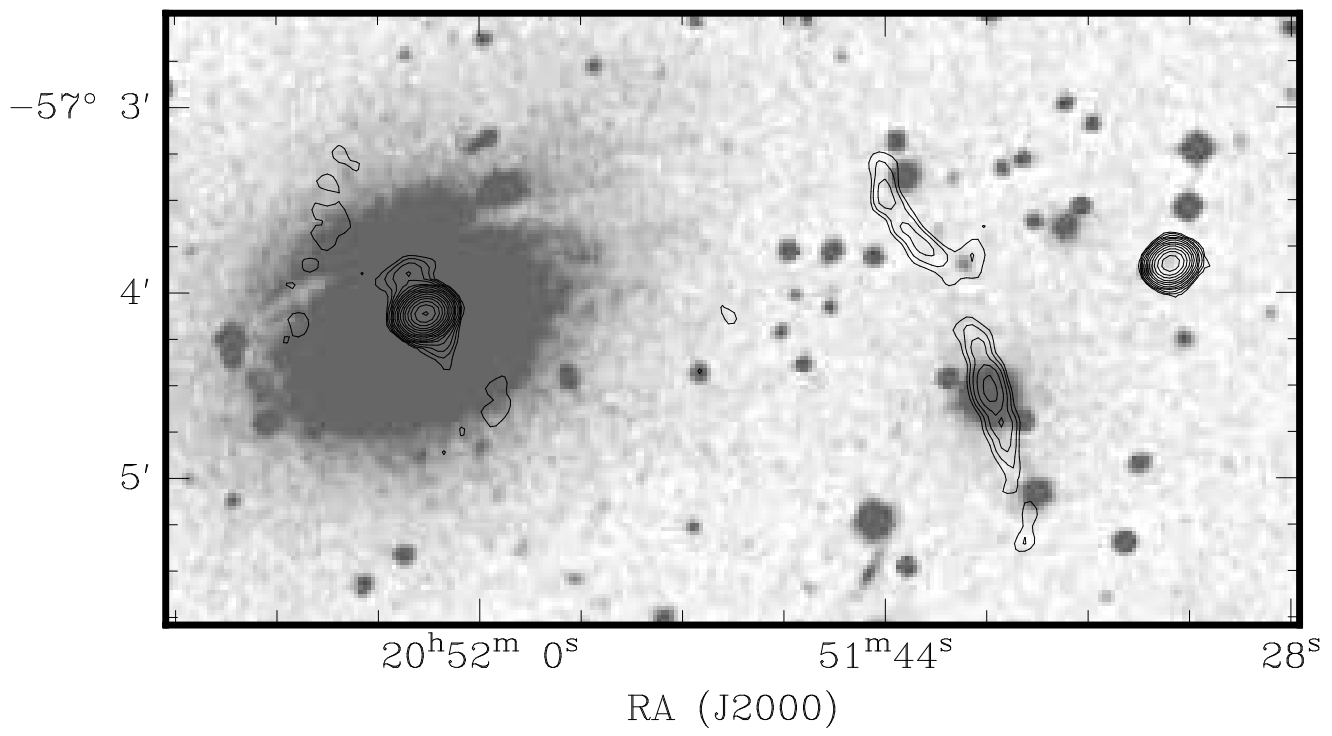
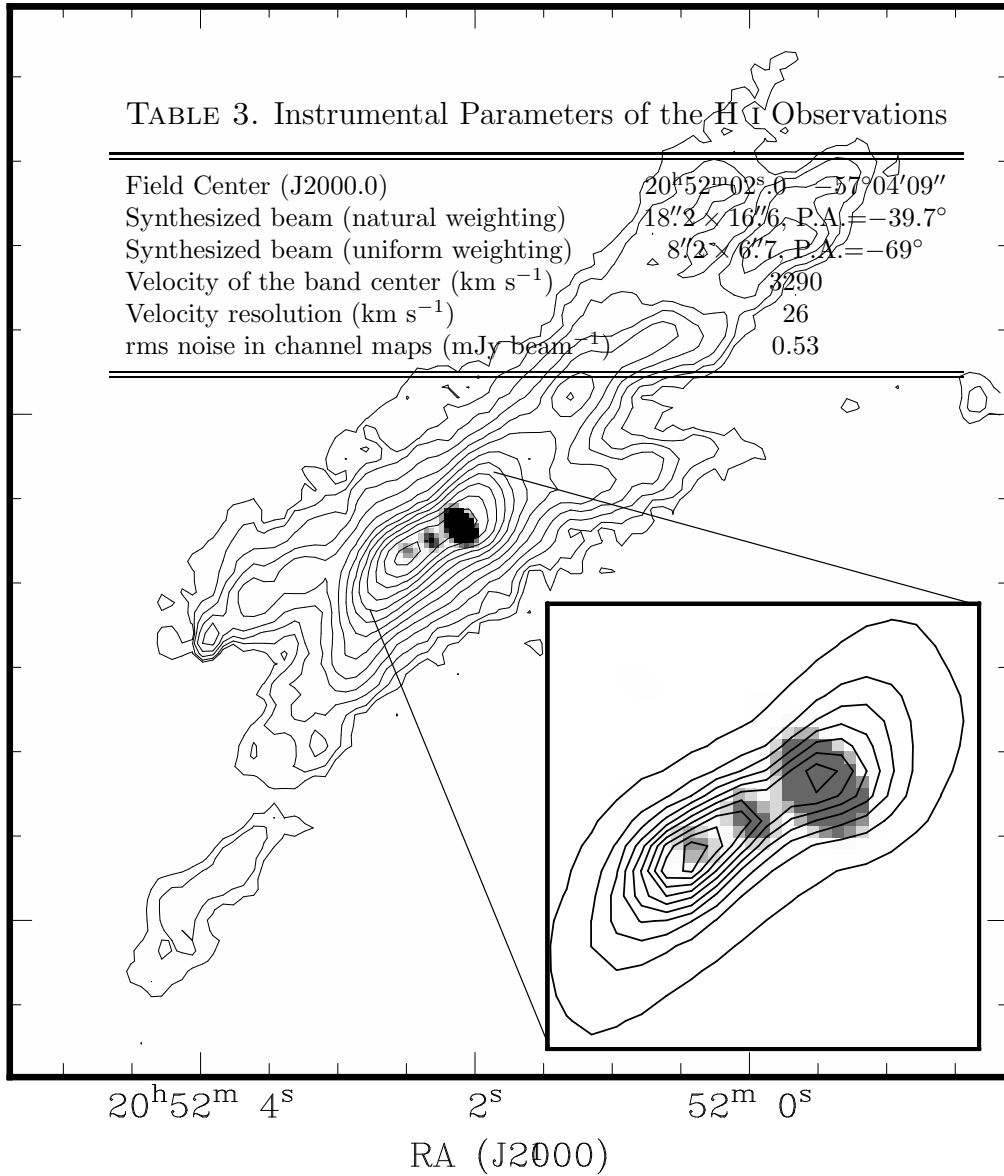
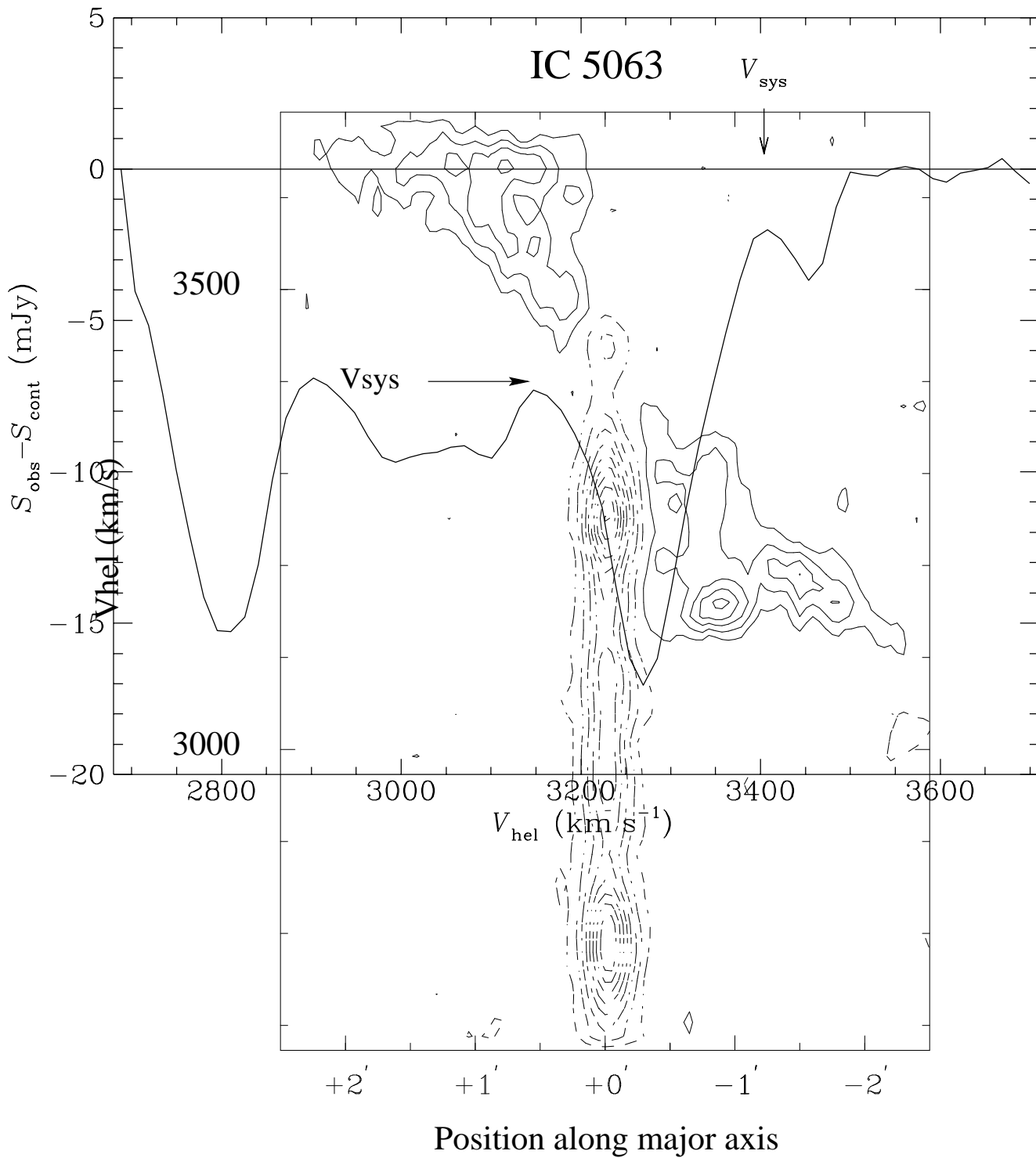


TABLE 2. H I Observations

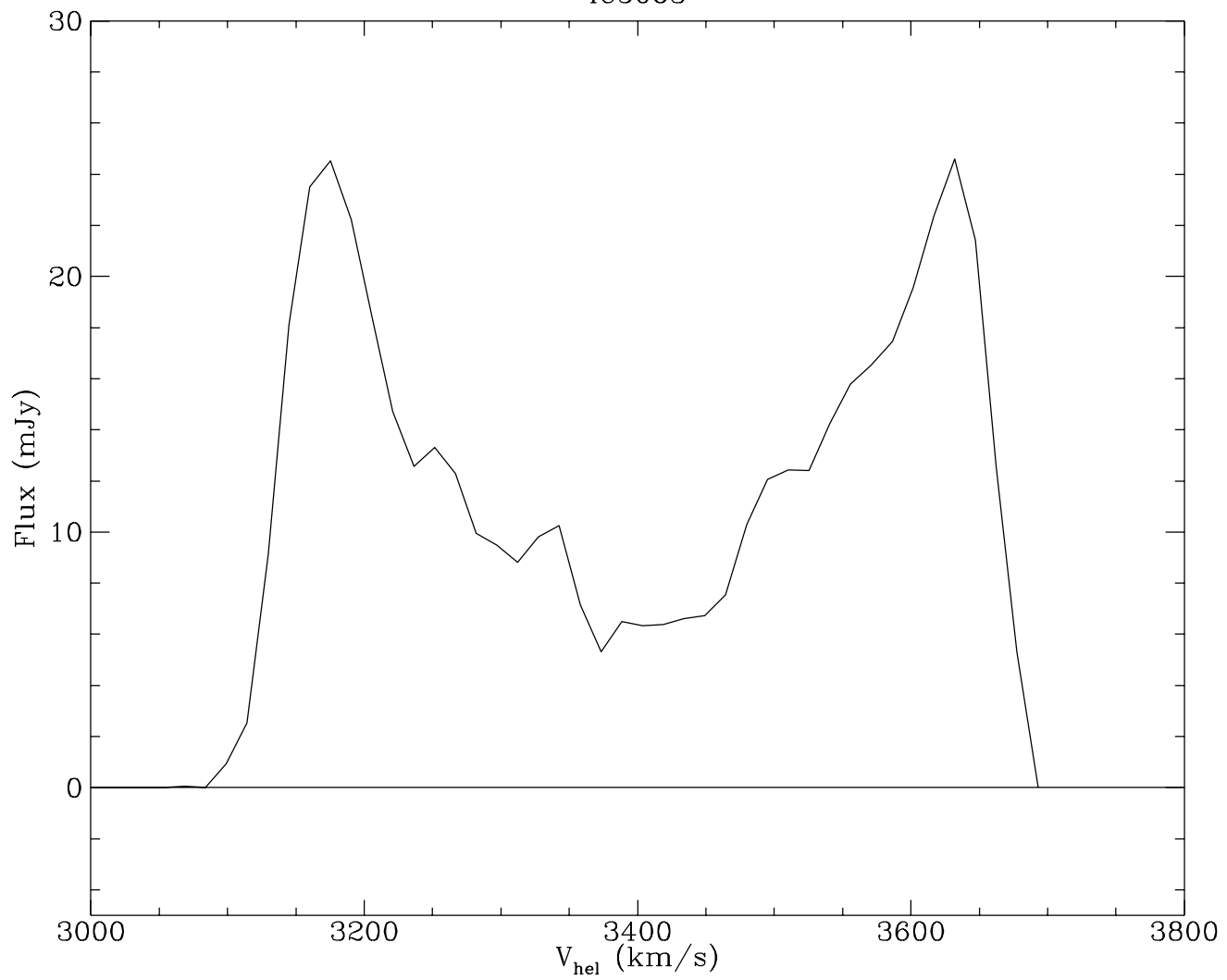
Date	ATCA Configuration	Min-Max Baseline (m)	Bandwidth (MHz) /channels	Frequency (MHz)	Time (h)
1995 Sep	750D	31–719(4469)*	16/256	1406	12
1995 Dec	6C	153–6000	16/256	1406	5
1996 Apr	6A	337–5939	16/512	1406	12
1996 May	1.5D	107–1439(4439)*	16/512	1406	12
1996 Jun	6D	77–5878	16/512	1406	12

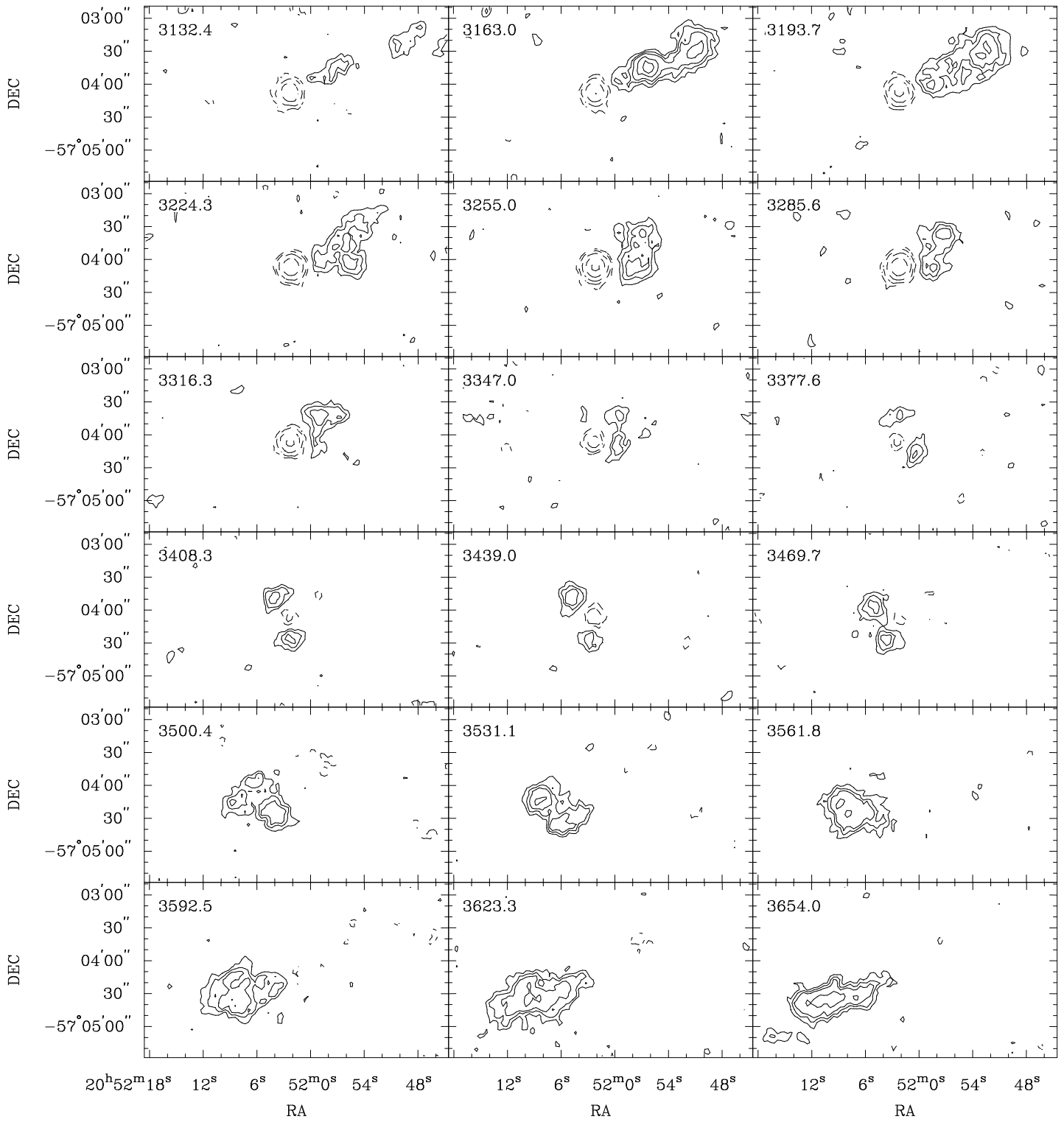
*the longest baseline length using also the 6 km antenna is given in parenthesis.

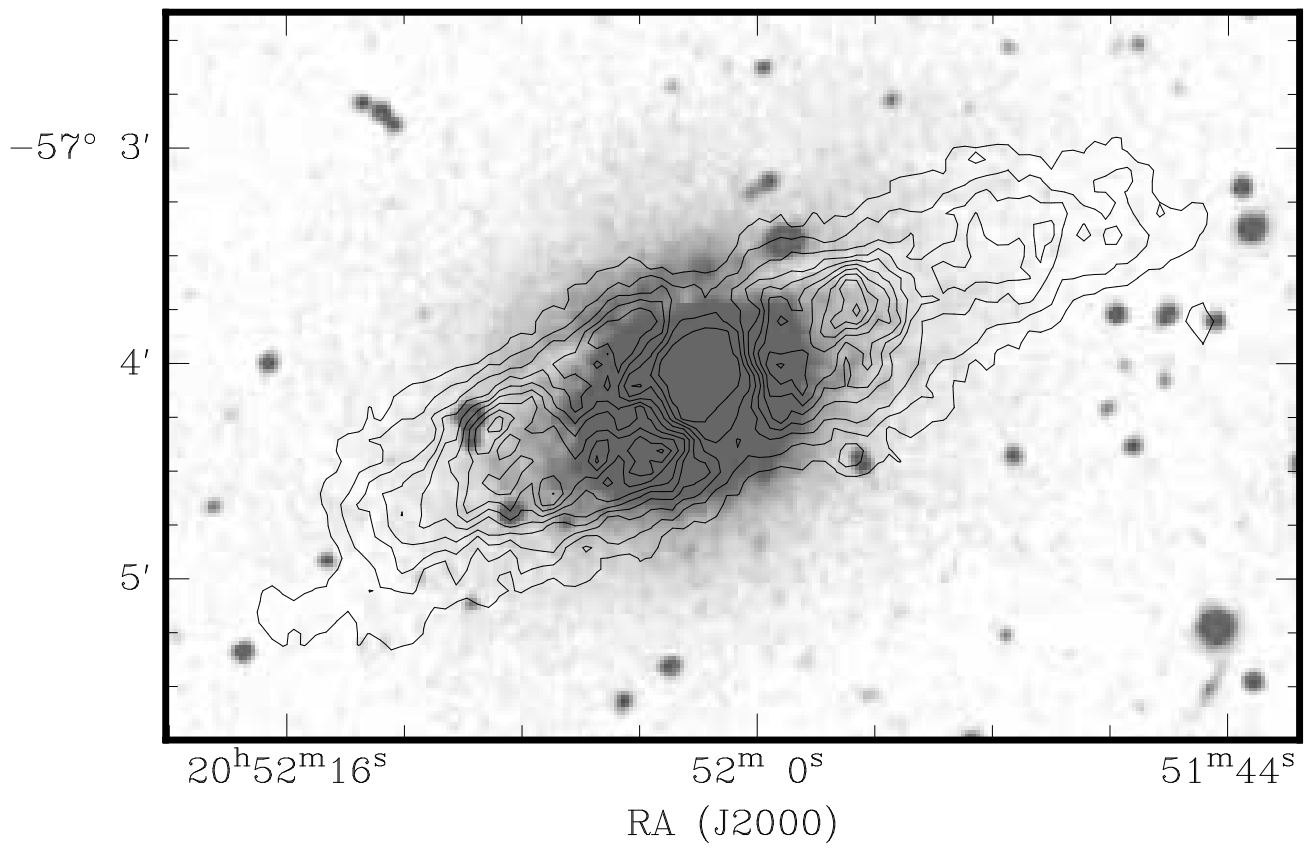




IC5063







This figure "Morganti.fig09.jpg" is available in "jpg" format from:

<http://arxiv.org/ps/astro-ph/9711285v1>

This figure "Morganti.fig10.jpg" is available in "jpg" format from:

<http://arxiv.org/ps/astro-ph/9711285v1>

This figure "Morganti.fig11.jpg" is available in "jpg" format from:

<http://arxiv.org/ps/astro-ph/9711285v1>

To appear in the *Astronomical Journal*, February 1998

A RADIO STUDY OF THE SEYFERT GALAXY IC 5063: EVIDENCE FOR FAST GAS OUTFLOW¹

R. MORGANTI

CSIRO, Australia Telescope National Facility, PO Box 76, Epping, NSW 2121, Australia
and Istituto di Radioastronomia, CNR, via Gobetti 101, 40129 Bologna, Italy

T. OOSTERLOO

CSIRO, Australia Telescope National Facility, PO Box 76, Epping, NSW 2121, Australia

Z. TSVETANOV

Department of Physics and Astronomy, Johns Hopkins University, Baltimore, MD 21218, USA

ABSTRACT

We present new radio continuum (8 GHz and 1.4 GHz) and H I 21 cm line observations of the Seyfert 2 galaxy IC 5063 (PKS 2048-572) obtained with the Australia Telescope Compact Array (ATCA). The high resolution 8 GHz image reveals a linear triple structure of $\sim 4''$ (1.5 kpc) in size. This small-scale radio emission shows a strong morphological association with the inner part of the optical emission line region (NLR). It is aligned with the inner dust lane and is oriented perpendicular to the position angle of the optical polarization. We identify the radio nucleus to be the central blob of the radio emission. At 21 cm, very broad ($\sim 700 \text{ km s}^{-1}$) H I absorption is observed against the strong continuum source. This absorption is almost entirely blueshifted, indicating a fast net outflow, but a faint and narrow redshifted component is also present. In IC 5063 we see clear evidence, both morphological and kinematical, for strong shocks resulting from the interaction between the radio plasma and the interstellar medium in the central few kiloparsecs. However, we estimate the energy flux in the radio plasma to be an order of magnitude smaller than the energy flux emitted in emission lines. Thus, although strong shocks associated with the jet-ISM interaction occur and could contribute locally to the ionization of the NLR, they are unlikely to account solely for the global ionization of the emission line region, particularly at large distances.

The main structure of the H I emission is a warped disk associated with the system of dust lanes of $\sim 2'$ radius ($\sim 38 \text{ kpc}$, corresponding to ~ 5 effective radii). The lack of kinematically disturbed gas (both neutral and ionized) outside the central few kpc, the warped structure of the large scale disk together with the close morphological connection between the inner dust lanes and the large-scale ionized gas, support the idea that the gas at large radii is photoionized by the central region, while shadowing effects are important in defining its X-shaped morphology.

From the kinematics of the ionized and of the neutral gas, we find evidence for a dark halo in IC 5063, with very similar properties as observed in some other early-type galaxies.

Subject headings: galaxies: individual (IC 5063) — galaxies: nuclei — galaxies: ISM — galaxies: Seyfert

¹Based on observations with the Australia Telescope Compact Array (ATCA), which is operated by the CSIRO Australia Telescope National Facility

1. INTRODUCTION

The narrow-line regions (NLR) in Seyfert galaxies occupy the central area in the host galaxy immediately surrounding the active nucleus. Observationally, these are regions of highly ionized gas at radial distances between ~ 10 pc (the *HST* resolution at 10–15 Mpc) to ~ 1 kpc from the nucleus. The NLRs are kinematically complicated and represent some of the best examples of regions where interaction between the local ISM and radio plasma takes place. The presence of such interactions was first inferred from ground-based optical spectroscopy of Seyfert galaxies with prominent linear radio sources. The emission lines in these regions usually have larger widths than implied by simple gravitational motion and often show kinematical splits as well as a morphological correspondence with the radio emission (e.g., Whittle et al. 1988).

In the past few years a number of Seyfert galaxies have been observed by the *HST* producing an impressive collection of images of their NLRs (see Wilson 1997 for a review; Capetti et al. 1996 and references therein). In some objects, the association between the radio plasma and the line emitting clouds is particularly striking. The ionized gas often appears to form a ‘cocoon’ around the radio emission. This supports the idea that the radio plasma compresses and heats the ISM that, cooling down, produces the NLR clouds. Shocks may, therefore, be very important in determining the kinematics, morphology and ionization state of the NLR.

In contrast, the extended emission line regions (EELR, Unger et al. 1987) are traced up to tens of kpc from nucleus, and appear to have a kinematically relaxed structure and no strong radio counterpart, although their symmetry axis is invariably aligned with the position angle (P.A.) of the elongated radio emission (Wilson & Tsvetanov 1994). The EELRs are believed to be mainly the result of photoionization by the UV radiation from the active nucleus and, if this is the case, the observed tight alignment implies that the radio plasma and the ionizing photons are collimated by the same or by strictly co-planar structures.

A careful comparison of the morphologies and kinematics of the gas in different phases is a key element in understanding the physics of NLRs in Seyfert galaxies. In this respect, obtaining the parameters of the neutral gas is of particular interest. High resolution H I observations give the distribution and kinematics of the *cold* component of the circumnuclear ISM and, therefore, complement the optical data. This has been done for a few objects. For example, by studying the neutral hydrogen in the center of NGC 4151, Pedlar et al. (1992) found a close agreement between the kinematics of the ionized gas and of the neutral hydrogen, strongly supporting the idea that the ionized gas is simply a component of the gaseous disk, ionized by an energy source in the nucleus. This supports the photoionization model and puts important constraints on the opening angle of the ionizing radiation from the nucleus. Additionally, H I absorption-line observations have the advantage of being able to clearly distinguish between infall and outflow of gas and provide us with information about the kinematics of the neutral gas along the line of sight to the radio continuum. In NGC 1068 and NGC 3079, high resolution H I observations (Gallimore et al. 1994) show evidence for wind-driven outflow, indicating that in these galaxies shocks could be important in determining the ionization structure of the gas. Similar observations have been done by Brinks & Mundell (1996).

To investigate these issues in more details, we have carried out a study of the nearby Seyfert 2 galaxy IC 5063 (PKS 2048-572). This object has a number of interesting characteristics among which (1) the Seyfert nucleus is hosted by an early-type galaxy, (2) it is particularly strong in the radio continuum ($P_{1.4\text{GHz}} = 6.3 \times 10^{23} \text{ W Hz}^{-1}$) allowing a comfortable study of the H I absorption and (3) it is rich in H I.

Despite these interesting characteristics, only a low resolution radio image (made with the Fleurs radio telescope) and a total H I profile (obtained with the Parkes radio telescope) are available for IC 5063

(Danziger, Goss & Wellington 1981, hereafter DGW81). In this paper we present new radio observations, both in the continuum and in the H I 21 cm line, obtained with the Australia Telescope Compact Array (ATCA). Our main goals are to map the morphology of the radio plasma on the kiloparsec scale and compare it with that of the ionized gas, and to study the kinematics of the neutral gas and compare it with that of the ionized gas.

The paper is organized as follows: the basic properties of IC 5063 are summarized in §2 and the radio observations and the data reduction are described in §3. In §4 we present the major observational findings and in §5 we discuss their consequences for understanding the physics of this complex system. Throughout the paper we adopt a Hubble constant of $H_0 = 50 \text{ km s}^{-1} \text{ Mpc}^{-1}$.

2. BASIC PROPERTIES OF IC 5063

IC 5063 is a nearby ($z = 0.0110$) early-type galaxy hosting a Seyfert 2 nucleus and has been studied in different wavebands. In the optical, the surface brightness distribution is well described by a $R^{1/4}$ law and, therefore, it can be classified as an elliptical or S0 galaxy. A gaseous disk is present and it has a complicated system of (major axis) dust-lanes (DGW81; Colina, Sparks & Macchetto 1991, hereafter CSM91). Moreover, the high contrast image of DGW81 shows faint structures in the outermost regions reminiscent of tidal arms. The optical spectra show strong emission lines (DGW81; Bergeron, Durret & Boksenberg 1983) with the ionized gas extending up to ~ 20 kpc and lying mainly in a disk (DGW81) but with anomalously high velocities observed near the nucleus. Bergeron et al. (1983) and CSM91 detected a faint, very broad emission-line component and Wagner & Appenzeller (1989) found an off-nuclear region with broad emission lines.

In polarized light IC 5063 shows high polarization in the near IR (Hough et al. 1987) and a strong, broad H α emission (Inglis et al. 1993). Like in some other Seyfert 2 galaxies this suggest that there is a broad-line region which is obscured from our direct view and the broad-line radiation is scattered into our line of sight by scatterers outside the obscuring regions. This is also suggested by the detection of hard X-ray emission (Koyama et al. 1992) viewed through a high column density ($N_{\text{H}} = 2 \times 10^{23} \text{ cm}^{-2}$) and with a X-ray luminosity and a spectral index in the range typically found for Seyfert 1 galaxies.

IC 5063 is a strong *IRAS* source (see Table 1) and has a warm far-infrared excess peaking at $60 \mu\text{m}$ (Heisler & Vader 1995). It has also been observed in CO by Wiklind et al. (1995) where it shows a narrow profile ($\Delta V_{\text{CO}} = 163 \text{ km s}^{-1}$).

Finally, the radio luminosity of IC 5063 is nearly two orders of magnitude larger than typical for nearby Seyferts (Wilson 1991), making it one of the strongest radio sources found in Seyfert galaxies. Because of this, it was suggested by CSM91 that this object may well represent an intermediate or transition type between Seyfert and radio galaxies. Also, its H I content is very high: DGW81 found $1.0 \times 10^{10} M_{\odot}$ that gives $M_{\text{HI}}/L_B = 0.19$, quite anomalous for such a type of object (Wardle & Knapp 1986).

The properties of IC 5063 are summarized in Table 1.

3. OBSERVATIONS

3.1. Radio continuum observations

IC 5063 has been observed with ATCA at 8 GHz to complement an optical narrow-band imaging survey of a distance limited sample of southern Seyfert galaxies (Tsvetanov, Fosbury & Tadhunter in prep., hereafter TFT; Morganti et al. in prep.). The observations were done in July 1995 using the 6 km configuration (the longest available with ATCA). We took data simultaneously at 8.256 and 8.896 GHz using a bandwidth of 128 MHz for each of these frequencies. These separate frequencies allowed us to improve (radially) the uv coverage. This is important in the case of ATCA because it is a six-telescope east-west array. We observed IC 5063 for about 6 hours in cuts of 15 min spread over 2×12 hours. The data reduction was done with the MIRIAD package (Sault et al. 1995) which is particularly well suited for ATCA data.

The 8 GHz image has a rms noise of $0.15 \text{ mJy beam}^{-1}$ with a beam shape of $1''.1 \times 0''.8$ elongated in position angle 51.8° . The resolution of this radio image is the highest reachable with ATCA and matches the resolution of the optical narrow-band images.

An image of the radio continuum was also made at 1.4 GHz by using the line-free channels in the H I line observations (see below) and combining the data from the 6 km (6D) and 750 m configurations (see Table 2). We obtained a rms noise of $0.8 \text{ mJy beam}^{-1}$ and a beam (using uniform weighting) of $8''.2 \times 6''.7$ (P.A. -69°).

3.2. H I Observations

As mentioned earlier, the aim of our H I observations is to investigate the properties of the neutral gas and compare them to those of the ionized gas. Given the extent of the ionized gas in IC 5063, we have mainly used the longer configurations available with the ATCA (6 km), but data with shorter configurations were also collected to improve the sensitivity for low surface-brightness extended emission. We have made images of the line data using both natural weighting (to study the overall distribution and kinematics of the H I) and uniform weighting (to study the H I near the center). Nevertheless, the final resolution of our H I data is still much lower than that of the optical data or of the 8 GHz radio continuum. The data reduction was done using MIRIAD and GIPSY (Allen, Ekers & Terlouw 1985). The configurations used as well as other observational parameters are summarized in Tables 2 and 3.

An interference spike generated by the data acquisition system is present at 1408 MHz, corresponding to a velocity of $\sim 2644 \text{ km s}^{-1}$ and therefore at the edge of the H I absorption profile of IC 5063 (see below). Although it limits slightly our ability to determine the exact extent of the absorption profile, it does not in any way affect the conclusions.

3.3. Optical imaging

IC 5063 was observed as part of a survey of volume limited sample of southern Seyfert galaxies (TFT). All images of IC 5063 were taken with the European Southern Observatory (ESO) Faint Object Spectrograph and Camera 1 (EFOSC1) attached to the 3.6 m telescope at La Silla, Chile, on 1993, July 14 and 15. The detector used was a Tek 512 CCD with ~ 7 electrons read-out noise. The pixel size of 27μ provided a scale of $0''.6075 \text{ pixel}^{-1}$ and just over $5'$ field of view.

The galaxy was imaged through filters isolating the redshifted positions of [O III] $\lambda 5007$ and $\text{H}\alpha + [\text{N II}]$

$\lambda\lambda 6548, 84$ emission lines (on-band) and their adjacent continua (off-band). The filters used have width of $\Delta\lambda \sim 60\text{\AA}$ and $\sim 70\text{--}80\text{\AA}$ in the [O III] $\lambda 5007$ and $H\alpha$ wavelength region, respectively. In the case of IC 5063 we took two exposures of 10 min per filter to allow for cosmic-ray hits cleaning afterwards.

The images were processed with the IRAF² software package. Reduction steps included: CCD bias subtraction, flat-fielding, and sky subtraction. The images were then registered using several well exposed stars in the field, and frames through the same filter were combined to clean the cosmic ray events and improve the signal-to-noise ratio. Small differences in the seeing were eliminated by convolving with a Gaussian to match the point spread functions (PSF). The final resolution of the of the IC 5063 images is $1''.7$ (FWHM).

Emission line maps were formed by scaling and subtracting the continuum images from the line+continuum ones. The scaling factors were determined from the emission-line free regions in the galaxy. Finally, the images were flux calibrated using the observations of spectrophotometric standard star through the same filters taken during the same night. We estimate that the overall flux calibration of the emission line maps is accurate to within 10%–15%. The noise level of individual frames is of order 10^{-17} ergs cm^{-2} s^{-1} px^{-1} .

4. RESULTS

4.1. The radio continuum

The 8 GHz radio continuum image is shown in Fig. 1. This image reveals a linear radio structure consisting of three clumps oriented in P.A. $\sim 295^\circ$. This morphology is common in Seyfert galaxies (Ulvestad & Wilson 1984, 1989). The total flux density at 8 GHz is 230 mJy ($\log P_{8\text{GHz}} = 23.11$ W Hz^{-1}) and the extent is about $4''$, corresponding to 1.3 kpc. Most of the flux (195 mJy) comes from the NW blob which clearly dominates the emission at that frequency. The central blob has a flux density of 16 mJy, while the eastern one is only 9 mJy. Despite the relatively high observing frequency, the blobs are unpolarized (we measure a fractional polarization of 0.5% only in the brightest blob). The low polarization is common in Seyfert galaxies, likely due to the Faraday depolarization from the dense gas around (Wilson 1991).

The line-free channels of the H I data have been used to make an image of the continuum emission at 1.4 GHz. The final map is presented in Fig. 2 superimposed onto the optical image from the Digitized Sky Survey (DSS) where the outer dust lane in IC 5063 is clearly visible. At 1.4 GHz we find a flux density of 1.26 Jy, in good agreement with the flux density derived by DGW81. Thus, our flux density measurement at 1.4 GHz (together with the data from literature), confirms the steep value of the overall spectral index ($\alpha \sim -1.1$ for $S \propto \nu^\alpha$) of IC 5063. Given that we have only one frequency (8 GHz) with sufficient resolution to separate the three blobs, we cannot estimate their spectral indices separately. The 21 cm radio continuum position is very close to that of the brightest 8 GHz blob (shifted slightly, by about $0''.5 \pm 0.04$, toward the east, see Fig. 1), indicating that also at 21 cm most of the flux comes from this region.

At 1.4 GHz the radio continuum is extended in a direction perpendicular to that at 8 GHz and it is roughly aligned with the minor axis of the galaxy and perpendicular to the dust lane. This emission, however, could be of different origin. Baum et al. (1993) have observed that the *large scale* radio structure in Seyfert galaxies is often aligned with the minor axis of the galaxy, and that this radio emission could be related to

²The Image Reduction and Analysis Facility (IRAF) is distributed by the National Optical Astronomy Observatories, which is operated by the Association of Universities for Research in Astronomy, Inc., under contract to the National Science Foundation

a starburst driven wind. They also find that in Seyfert galaxies the *small scale* radio structure in general has no correlation with either the large scale radio structure or with the optical orientation of the galaxy. It appears that IC 5063 behaves in a similar way. However, in active galactic nuclei hosted by early-type galaxies the radio emission is usually perpendicular to the dust lane (Kotany & Ekers 1979, Möllenhoff, Hummel & Bender 1992, van Dokkum & Franx 1995). This has been used to support the idea that the gas could fuel the activity in an active nucleus (Kotany & Ekers 1979), although a number of exceptions exist (Möllenhoff, Hummel & Bender 1992).

Finally, the position angle of the inner radio structure appears to be approximately perpendicular to that of the optical polarization (P.A. 34° , Inglis et al. 1993) as expected if the optical emission (in this case from the broad-line region) is scattered into the line of sight by electrons and/or dust grains. This is therefore in agreement with the prediction from the unified schemes.

The comparison between the radio and the ionized gas is of interest. The new optical narrow-band images (TFT) confirm the original result of CSM91 that the high-ionization line-emitting gas has an “X-shaped” morphology and show that the ionized gas can be traced out to a distance larger than $\sim 30''$. There are three radial filaments of highly ionized gas elongated along P.A. $285^\circ - 290^\circ$, P.A. $310^\circ - 315^\circ$, and P.A. $325^\circ - 330^\circ$. The basic symmetry axis of these extended emission line regions is roughly coincident with the major axis of the light distribution (P.A. $\sim 303^\circ$). The opening angle of the X-shaped structure is $\sim 50^\circ$.

The overlay of the 8 GHz map to the [O III] $\lambda 5007$ image from TFT is presented in Fig. 3. The radio emission is closely aligned with the symmetry axis of the ionized gas. For a sample of Seyfert galaxies, Wilson & Tsvetanov (1994) have found a tight alignment between the “ionization cone” and the radio axis. This seems to be the case also in IC 5063, although the ionized gas is in a X-shaped structure more than in a cone. Moreover, if we concentrate on the inner optical region we can see that the radio and optical structures are very similar as shown in the enlargement in Fig. 3. This is not really surprising given that it is well known that the NLR (i.e. ionized gas on the scale of few kpc) is invariably co-spatial with the radio emission (Wilson & Ulvestad 1983; Haniff, Wilson & Ward 1988).

An *HST* image of IC 5063 has been obtained from the the public archive. This image is a single 500 s exposure obtained with WFPC2 through filter F606W and shows even more impressively the complicated structure of the dust lane in the central region (see Fig. 11 insert). Already from the ground-based optical images, CSM91 described the dust lanes in IC 5063 as a “complicated zig-zagging distribution running approximately parallel to the major axis and mainly concentrated in the northern side and most symmetric nearest the nucleus”. As we discuss briefly in §5.4, the observed morphology can probably be explained as the result of a warped structure.

The insert in Fig. 11 shows the radio map at 8 GHz superposed onto the *HST* image. Given that the F606W filter includes bright emission lines ([O III] $\lambda 5007$, $H\alpha$ and [N II] $\lambda\lambda 6548, 84$), the observed morphology is strongly influenced by the emission-line gas. The overlay shows that the central radio blob corresponds to the peak of the light distribution. Although there is, as always, some uncertainty in the alignment of these images, the error in the relative positioning is at most $0''.5$. Comparing the 8 GHz image with the ground based [O III] $\lambda 5007$ image as well as the ground based [O III] $\lambda 5007$ image with the *HST* image, we can exclude that the brightest radio blob corresponds to the center of the galaxy. More difficult, also because of the low resolution of our radio image, is to say if the optical emission really “wraps around” the radio blobs like in a number of other Seyfert galaxies that have been studied at high resolution (e.g. Mrk 3, Capetti et al. 1995), although data suggests that also in IC 5063 this may be the case. We have obtained higher resolution VLBI radio data to investigate the small scale structure of the radio emission and

to attempt a better comparison with the structure of the ionized gas on the scale of the *HST* observations. Results from the VLBI observations will be presented in a future paper.

4.2. The Neutral Gas

In our study of the neutral gas in IC 5063 we detect the H I 21 cm line in absorption as well as in emission. These correspond to two very different components, both kinematically and spatially, of the local ISM and we discuss them separately below.

4.2.1. The H I absorption

The most striking feature in the H I data is the presence of very wide, mostly blueshifted absorption against the central continuum source. The position-velocity map taken along the major axis (Fig. 4) outlines the individual features of this broad absorption particularly well. The absorption profile is very broad ($\sim 700 \text{ km s}^{-1}$, because of the interference at 1408 MHz, corresponding to 2644 km s^{-1} , the accuracy of this determination is somewhat compromised), and almost entirely blue shifted, far beyond the velocities characteristic of the H I emission. The large velocity range and the asymmetry makes it unlikely that the motion is gravitational. Instead, it is more likely that we see a strong net outflow. The shape of the absorption profile (Fig. 5) suggests that there are several H I clouds along the line of sight, the main clouds being roughly 600 km s^{-1} and 150 km s^{-1} from the systemic velocity. A faint redshifted component is also visible.

It is important to remember that even in the 21 cm images made with uniform weighting, the achieved resolution is $\text{FWHM} \sim 7''$ and the central continuum source is only slightly resolved. Therefore, we cannot make a detailed determination against which of the three blobs observed at high frequency the absorption is occurring. However, averaging the line channels containing only H I absorption of the uniformly weighted data, the position of the absorption appears to be offset by $0''.5$ W with respect to the peak of the continuum at 21 cm and appears to be coincident with the position of the brightest blob in the 8 GHz map (see Fig. 1). This would mean that *at least the very blueshifted absorption is not against the nucleus but against the W blob*. We have estimated the level of significance of this apparent offset by means of a Monte Carlo simulation. We have made a large number of model images containing a point source of the appropriate strength and noise level. Fits to these model images indicate that the probability that the observed offset is due to noise effects is 4%.

This offset is in agreement with results from optical observations. In the region $\sim 2''$ NW from the center of the galaxy, i.e., co-spatial with the brightest radio knot at 8 GHz, Wagner & Appenzeller (1989) found unusually broad wings (several hundred km s^{-1}) of the permitted as well as forbidden lines. The peak of these broad profiles appears blueshifted by $\sim 150 \text{ km s}^{-1}$ with respect to the systemic velocity, with wings out to velocities similar to what we observe in the H I absorption. Wagner & Appenzeller (1989) interpreted these broad lines as nuclear emission scattered into the line of sight, although they could not rule out gas outflow. However, given the H I absorption we observe, gas outflow becomes the more likely hypothesis to also explain the optical observations. This strongly suggests that in the region of the brightest radio blob at 8 GHz a strong interaction between the radio plasma and the ISM takes place.

In the channels where there is both absorption and emission, the position of the absorption shifts towards

the peak of the 21 cm continuum, but this is (at least partially, perhaps completely) due to confusion with the H I emission.

4.2.2. The H I emission

IC 5063 contains an unusually large amount of H I for a galaxy of its type. We estimate $8.4 \times 10^9 M_{\odot}$ of H I over a wide velocity range: from ~ 3150 to ~ 3650 km s $^{-1}$. The global H I profile is shown in Fig. 6. The difference with the value obtained from Parkes observations ($10^{10} M_{\odot}$, DGW81) is very small and likely due to the relatively high resolution of our observation. Because the aim of our H I observations is to investigate the kinematics of the neutral gas and compare it with that of the ionized gas, the combination of arrays used in this work is not the most suitable for mapping very extended low-surface brightness H I emission. A proper study of the large scale characteristics of the H I emission is being carried out by Blank et al. (in prep).

The position-velocity map along the major axis (P.A. 120°) is shown in Fig. 4. This plot shows that, to first order, the H I is in a regularly rotating disk with systemic velocity of ~ 3400 km s $^{-1}$.

Figure 7 shows images from the individual velocity channels (plotted every second channel). Because of the strong absorption, the maps of the total intensity and the intensity-weighted mean velocity of the H I emission were made in the following way. The line maps were smoothed spatially to a resolution of 30 arcsec, after the negative values corresponding to the absorption were set to zero. This smoothed cube was used to mask the original cube: pixels with signal below 2σ in the smoothed cube were set to zero in the original cube. The total intensity image and the velocity field were derived from this masked version of the full resolution data. Fig. 8 shows the total H I intensity map of IC 5063 superimposed on the optical image of the galaxy. The “hole” in the center of the H I distribution (and coincident with the center of the galaxy) represents the region of strong absorption against the radio continuum.

The total H I intensity image and the velocity field (Fig. 10) show that the main structure of the H I emission is that of a disk, oriented in a direction very similar to the system of dust lanes (as in the majority of the dust-lane ellipticals with H I, Morganti, Sadler & Oosterloo 1997). We find that the H I emission extends to $\sim 2'$ radius, corresponding to just over 5 effective radii ($R_{\text{eff}} = 22''.4$; CSM91). The pattern of the dust lanes in IC 5063 already suggests that this galaxy contains a warped disk (e.g. DGW81). A number of dust lanes are in fact evident, each having a slightly different orientation, suggesting that IC 5063 is perhaps to some extent similar to galaxies like NGC 4753 (Steiman-Cameron, Kormendy & Durinsen 1992) where there is strong evidence for a gaseous disk precessing differentially in the potential of the galaxy. The H I velocity field confirms that the disk in IC 5063 is warped in a way one would expect from the morphology of the dust-lanes. From Fig. 4b in CSM91 one can see that there are three major dust-lanes: one close to the center, an intermediate dust-lane, making an angle of about 20° with the inner dust-lane, and an outer dust-lane that is more or less parallel with the inner one. The change in kinematic position angle that is evident in the velocity field corresponds to the change in orientation between the intermediate and outer dust-lane. Also at other positions (e.g. $\sim 30''$ east of the center) the velocity field shows kinks in the velocity contours, also characteristic of a warp.

4.3. Nearby objects

DGW81 reported one other radio source about $4'$ west of IC 5063. This object was also observed at 843 MHz by Jones & McAdam (1992) and is part of the Molonglo catalogue of radio sources (MRC 2047–572) and appears to be unrelated to IC 5063. MRC2047–572 is also visible in our 1.4 GHz image (see Fig. 2). From our data the position of this radio source can be determined much more accurately, and we now find marginal evidence for an optical identification for this source. The higher resolution of our data shows that the extension observed in this source by both DGW81 and Jones & McAdam (1992) actually consists of two (background?) radio sources. In Fig. 2 we show an overlay of the 1.4 GHz image on top of the optical image taken from the Digitized Sky Survey, showing the two radio sources just east of MRC 2047–572. This figure also shows that there is a background group or cluster of galaxies near IC 5063 with which these radio sources are possibly associated (as perhaps also their morphology suggests). From our data we obtained a flux of 320 mJy for MRC 2047–572 and ~ 97 mJy for the two other sources together. Comparing this with the flux derived from MOST observations (870 mJy, Jones & McAdam 1992) that includes all these sources, we obtain a steep overall spectral index of $\alpha \sim -1.4$.

We do not detect H I emission from any other object in the field.

5. DISCUSSION

5.1. The Strong Nuclear Outflow

There is a growing body of evidence that nuclear gas outflows are common in AGNs. In type 1 Seyfert galaxies, where our view of the nucleus is relatively clear, these are detected through absorption on the line of sight to the central UV and/or X-ray source. Recent *HST* observations indicate that at least 50% of Seyfert 1 galaxies have intrinsic UV absorption lines (e.g. Grenshaw 1997). Despite the small number of objects for which this data is available so far, a number of common properties are emerging. In all cases, the UV absorption is blueshifted (up to -1500 km s $^{-1}$ relative to systemic) indicating a net outflow. The absorption profiles are often broad (a few hundred km s $^{-1}$) and consist of multiple components suggesting macroscopic bulk motions. Absorption lines from elements and ions covering a large range of ionization stages have been detected. In the best studied cases such as NGC 4151 (Kriss et al. 1992) and NGC 3516 (Kriss et al. 1996), where spectra from the Hopkins Ultraviolet Telescope (*HUT*) and *HST* are available, these include hydrogen Lyman series, and ionization stages as high as O VI. A number of attempts have been made to relate the UV absorbers to the warm absorbers (cf Nandra & Pounds 1994) seen in the X-ray spectra of many Seyfert galaxies (Mathur 1994; Mathur et al. 1995), but it is clear that the single zone model is an oversimplification (e.g. NGC 3516; Kriss et al. 1996).

In Seyfert 2 galaxies the nucleus is obscured at all wavelengths from the near IR to the soft X-rays, and the evidence for outflows is mostly indirect. The outflows are inferred mainly from the detection of asymmetric wings and/or splitting of the lines from the resolved emission-line structure often associated with the radio emission (Whittle 1989; Unger et al. 1987). More recently, detailed multislit spectroscopy (e.g. Mulchaey et al. 1992) and/or integral field spectroscopy (Arribas et al. 1997 and references therein) of EELR in nearby Seyferts have yielded similar results. A number of good examples are summarized in Aoki et al. (1996).

Mapping the H I velocity profiles offers an opportunity to detect outflows unambiguously in Seyfert 2's and to compare the kinematics of neutral and ionized fractions in Seyfert 1's. The striking result about

IC 5063 is that such broad absorption does not seem to be at all common in Seyfert 2 galaxies, with the exception of NGC 1068. Clearly this broad absorption is the result of an interaction of a nuclear outflow with the gas in the circumnuclear ISM. However, the picture is further complicated by the fact that at least the most blueshifted absorption in IC 5063 is not against the nucleus but against the western radio blob (see §4.3 and Fig. 1). The situation is not like in NGC 1068 (Gallimore et al. 1994) where the more blueshifted absorption is seen against the core while the absorption against the jet is less blueshifted. Clearly, VLBI observations are needed to confirm our findings, and they will likely have to be combined with high resolution UV (*HST*) and X-ray observations to try to unravel this complex kinematics.

The H I column density we derive from the absorption profile is $N_{\text{HI}} = 1.0 \times 10^{21}$ atom cm^{-2} , assuming a spin temperature $T_{\text{spin}} = 100$ K. This value of N_{HI} is very similar to the column densities found in other Seyfert galaxies (also assuming $T_{\text{spin}} = 100$ K): $(3.9 \pm 0.5) \times 10^{21}$ atom cm^{-2} for NGC 4151 (Mundell et al. 1995), and $(1 - 4) \times 10^{21}$ atom cm^{-2} for NGC 1068 (Gallimore et al. 1994). However, the column density we derive is likely to be a lower limit for several reasons. First, given the relatively low resolution, the absorption is likely to be confused by some H I emission from the disk. Second, in estimating the optical depth, we have assumed that the absorption is uniform over the continuum source. It is, however, possible that the absorption is seen against only one or two of the blobs observed at 8 GHz, and perhaps we even see evidence for that (see §4.3). This would lead to underestimating the optical depth. Let us for the sake of argument assume that the structure in the continuum at 21 cm on an arcsecond scale consists also of 3 blobs. Then if all the absorption is against the brightest radio source, the above column density would not increase significantly, since most of the 21 cm flux comes from that blob. In the extreme case where the absorption is against the core, the estimated column density would depend strongly on the spectral index one wants to assign to the core. If we assume a flat spectral index for the core, the optical depth becomes very high given that the core flux (16 mJy) would be the same as the strength of the absorption. In the case of a steep spectral index (e.g., $\alpha = -1$) the core flux would be ~ 100 mJy and the column density would become 1.3×10^{22} atoms cm^{-2} . Only higher resolution observations could clarify this point.

Finally, and probably most importantly, the presence of a strong continuum source near the H I gas may significantly increase the spin temperature because in this case the radiative excitation of the H I hyperfine state can dominate the usually more important collisional excitation (e.g., Bahcall & Ekers 1969). We have estimated the magnitude of this effect and find for a wide range in volume densities of the H I that if the absorbing H I gas is closer than about 500 pc from the strongest radio source, the spin temperature is at least several thousand Kelvin. So it is quite likely that the column density corresponding to the H I absorption is at least 10^{22} cm^{-2} , while it is not even impossible that it is as high as $\sim 10^{23}$ cm^{-2} , similar to what is derived from X-ray observations (Koyama et al. 1992).

The redshifted component of the H I absorption might be associated with a nuclear torus/disk. The width of the CO profile as observed by Wiklind et al. (1995) is very narrow compared to the total H I emission profile. This clearly means that the CO emission does not come from the molecular counterpart of the H I disk. Assuming that the range of velocities in the CO is due to rotation, the inclination of the CO disk must be quite different from that of the H I disk. Interestingly, the half-width of the CO profile (82 km s^{-1}) corresponds quite closely to the width of the redshifted absorption component, suggesting perhaps that both originate in the same structure.

The blueshifted absorption observed in IC 5063 is also very unusual when compared to other nearby elliptical galaxies (of which none have a Seyfert nucleus) that have nuclear sources of comparable radio power. In these nearby elliptical galaxies, if absorption is observed against the central continuum source, this absorption is invariably redshifted and is much narrower in velocity, as found by van Gorkom et al. (1989).

Narrow absorption has also been detected in a number of more powerful radio galaxies (Cygnus A, Conway & Blanco 1995; Hydra A, Dwarakanath, Owen & van Gorkom 1995 and NGC 4261, Jaffe & McNamara 1994). The fact that, on the contrary, IC 5063 shows the broad blueshifted absorption could be due to some stronger kind of interaction going on in this object, possibly because of the richer ISM. This could be related to the fact that the radio jet is aligned with the dust-lane, i.e. it escapes the nucleus in the direction of the disk of gas and therefore the interaction between the radio plasma and the environment is particularly strong.

5.2. Shocks in the NLR

The radio source in IC 5063 is unusually strong when compared to those observed in typical Seyfert galaxies. Nevertheless, IC 5063 exhibits characteristics similar to those of other Seyfert galaxies studied at radio wavelengths. In particular, the linear radio structure is only a few kpc in size, it is coincident with the inner, bright, part of the optical emission line region, and its position angle is very close to the symmetry axis of the extended emission line region.

The comparison of the 8 GHz radio map with the *HST* image (Fig. 11) reveals morphological characteristics similar to what is observed in other Seyfert galaxies with close association between radio and line emission. Although the uncertainty in the alignment of the radio and *HST* images does not warrant a detailed investigation, the optical emission could be “wrapping around” the radio blobs as found in cases like Mrk 3 (Capetti et al. 1995). Because of this close association, the structure of the line emitting gas in the NLR of IC 5063 is likely to be dominated by the compression and heating of the interstellar gas generated by shock waves produced by the supersonic radio plasma.

The presence of strong outflow in IC 5063 also suggests strongly that fast shocks driven by the radio plasma must be present in the circumnuclear region. This raises the usual question of the importance of shocks as ionization mechanism in Seyfert galaxies. Models involving bow shocks driven into the circumnuclear medium by radio jets have been proposed by Pedlar, Dyson & Unger (1985) and Taylor, Dyson & Axon (1992). These models generate high velocities and large velocity dispersions in the line emitting gas, but continue to rely on UV radiation from the nucleus to ionize the gas compressed by the shocks. More recently, Dopita & Sutherland (1995, 1996) have suggested that radiation from the shocks themselves plays the dominant role in the ionization of the line emitting gas.

We have used energy budget arguments to investigate if the energy supplied by the radio plasma is sufficient to explain the energy radiated in the emission lines. Following the calculations presented by Bicknell (1995), we find that the energy flux derived from the radio (using our 8 GHz data) is $\sim 2 \times 10^{42}$ ergs s^{-1} . The observed [O III] $\lambda 5007$ luminosity is $L_{[\text{O III}]}$ = 6.6×10^{41} ergs s^{-1} (CSM91) and the great majority of this is coming from the central region coincident with the radio emitting region. The total line luminosity can be estimated to be about 10–15 times the [O III] $\lambda 5007$ luminosity. Clearly, unless the radio lobes are well out of equipartition or the lobe plasma contains a significant thermal component (Bicknell et al. 1998), the radio energy is not sufficient to completely power the line emission. As the broad H I absorption shows, fast shocks do occur in IC 5063 and they could be important for the ionization locally (similar to as was shown to be the case in NGC 1068; Capetti et al. 1997), but it seems that for the ionization of the NLR of IC 5063 the UV photons from the active nucleus are also required. This appears to be observed in basically all Seyfert galaxies (Bicknell et al. 1998).

We also note that the brightness distribution of the optical emission line gas in the central few kpc is

quite symmetrical with respect to the center, while the radio emission is very asymmetric. This also suggests that the interaction between the radio plasma and the surrounding gas is not the only mechanism responsible for the ionization of the NLR.

5.3. Shadowing and ionization from nucleus

The other interesting aspect of our observations is the relationship between the ionized gas and the neutral gas we see in emission. Outside the central region where the absorption occurs, the kinematics of the H I is very regular and there are no indications for interaction between the radio plasma and the H I disk. Thus, the interaction between radio and ISM appears to be confined to the central region. Given that the H I appears to fill the disk rather well, the sharp and straight edged structure of the ionized gas must be connected with the shape of the radiation field (typical of photoionization, Morse et al. 1996). A comparison of the morphology of the highly ionized gas (e.g., ratio [O III] $\lambda 5007/H\alpha$) with that of the inner dust structures visible in the *HST* image, combined with the fact that the gas disk in IC 5063 is warped, reinforces the suggestion of CSM91 that shadowing effects are important and that the gas at larger radii is photoionized by the central UV source. This is illustrated in Fig. 11 where we have overplotted the distribution of the high-excitation ionized gas (as derived from the [O III] $\lambda 5007/H\alpha$ ratio map from TFT) onto the *HST* image. As noted before by CSM91, the location of the inner dust lane is very suggestive for the morphology of the high-excitation gas being determined by shadowing effects caused by the inner dust lane.

Figure 9 shows the total H I superimposed to the [O III] $\lambda 5007$ image. The extent of the ionized gas coincides very well with that of the H I disk. The H I velocities near the center (see the position-velocity map in Fig. 4) also correspond exactly to the velocities of the ionized gas measured by DGW81 and CSM91 along the major axis of the ionized gas distribution. The neutral gas does not appear to be disturbed in the region outside the inner few kpc. This suggests that in IC 5063 we are observing a situation similar to NGC 5252 (Prieto & Freudling 1993, 1996). Based on images of the H I, combined with narrow-band images and kinematical information of the ionized gas, Prieto & Freudling concluded that in NGC 5252 there is single gas system which is only partly ionized because of the anisotropy of the ionizing radiation. The fact that in IC 5063 the ionized gas has the same extent as the H I, and the kinematics of the two appear to connect smoothly, suggest that also in this object the neutral and the ionized gas are physically connected. For NGC 5252, Prieto & Freudling (1996) argued that the fact that both physical states can exist at a similar distance from the nucleus implies that the radiation field must be anisotropic. It appears that this argument also applies to IC 5063.

5.4. The H I disk and its origin

The H I emission is extended in the direction of the dust-lane. This has been found in most of the dust-lane ellipticals that show H I emission (Morganti, Sadler & Oosterloo 1997; also NGC 1052, van Gorkom et al. 1986, and Centaurus A, van Gorkom et al. 1990).

As for all the early-type galaxies with a detectable amount of H I, the origin of the neutral gas in IC 5063 is believed to be external due to a merger with a gas-rich galaxy. The merger hypothesis for IC 5063 has been already suggested both by DGW81 and CSM91 for a number of reasons. For example, the fact that dust lanes appear to be more symmetric near the center supports the idea of an external origin for the dust. As in

the case of e.g. NGC 5266 (Morganti et al. 1997) the amount of H I present in IC 5063 is atypical for a galaxy of its type, the observed M_{HI}/L_B is more characteristic of a late-type spiral. Therefore, the origin of the H I in IC 5063 is very likely a merger between two (or more) spiral galaxies, not just an accretion of a small gas-rich object. The effect of this event can be seen also from the faint optical “tails” observed by DGW81 in their deep optical image. Our data do not have the right combination of resolution and sensitivity to find a possible low-surface-brightness H I counterpart of these faint optical tails, as is observed in e.g. NGC 5266 (Morganti et al. 1997) or in some shell galaxies (Schiminovich et al. 1995)

Most of the neutral gas appears to be in a disk, suggesting that the gas is settled and the merger is relatively old. Because of this, we can make an estimate of the M/L for IC 5063 at large radius. We estimate the projected rotation velocity to be about 240 km s^{-1} . Assuming a spherical mass distribution, this gives a $M/L_B \sim 14$ at $5.4 R_{\text{eff}}$, where we have assumed an inclination of 74° as determined from the axial ratio of the H I disk. The optical data of DGW81 and of CSM91 show that at small radii the rotation velocity is very similar to that estimated from the H I in the outer regions, so the rotation curve of IC 5063 appears to be quite flat. Assuming a flat rotation curve, we find for the mass-to-light ratio at $1.3 R_{\text{eff}}$ (i.e. the radius out to which velocities can be measured from the optical data) a value of $M/L_B \sim 5$. We have not taken into account the fact that the inclination of the inner disk could be slightly different from that of the outer disk, but this can have only a small effect on our estimates of M/L , since this inclination is in any case relatively large. We have also neglected possible effects due to non-circular orbits related to a possibly triaxial potential in IC 5063, but it appears that the increase of M/L_B with a factor of almost 3 does point to the presence of a halo of dark matter in IC 5063. The observed values for M/L_B in IC 5063 quite accurately follow the trend of M/L with radius noted for other early-type galaxies by Bertola et al. (1993).

6. CONCLUSIONS

We have presented radio continuum and H I observations of the Seyfert 2 galaxy IC 5063 to investigate the ionization mechanism in the NLR as well as the kinematics of the gas in different phases. The high resolution of our 8 GHz image reveals a linear structure that presents strong morphological association with the NLR and is aligned with the optical dust lane.

Very broad ($\sim 700 \text{ km s}^{-1}$) H I absorption is observed against the strong continuum source, indicating a fast net outflow. This outflow, together with the morphological correspondence between the radio emission and the NLR, represent a strong argument for the presence of shocks resulting from the interaction between the radio plasma and the interstellar medium in the inner few kpc. Nevertheless, the energy flux estimated from the radio emission is not enough to power the emission of the optical lines. Although the morphology and the broad H I absorption suggest that shocks play a role at some level locally, UV photons from the active nucleus are necessary to explain the ionization of the NLR.

The main structure of the H I emission is a warped disk. Shadowing effects from this disk are likely to be important in explaining the morphology of the EELR. Moreover, the neutral gas does not appear to be kinematically disturbed outside the inner few kpc – the kinematics of the H I connects smoothly that of the ionized gas in the center. This indicates that both the ionized and neutral gas components are just different phases of the same structure and this argues in favour of an anisotropic radiation field responsible of the EELR morphology.

From the kinematics of the ionized and of the neutral gas, we find evidence for a dark halo in IC 5063, with very similar properties as observed in some other early-type galaxies.

This research has made use of the NASA/IPAC Extragalactic Database (NED) which is operated by the Jet Propulsion Laboratory, Caltech, under contract with NASA. The Digitized Sky Survey (DSS) was produced by the Space Telescope Science Institute (STScI). The DSS is based on photographic data from the Oschin Schmidt Telescope, which is operated by the California Institute of Technology and Palomar Observatory, and the UK Schmidt Telescope, which is operated by the Royal Observatory Edinburgh, the UK Science and Engineering Research Council and the Anglo-Australian Observatory. ZT acknowledges support from NASA LTSA grant NAGW-4443 to the Johns Hopkins University.

REFERENCES

- Allen, R. J., Ekers, R. D., & Terlouw, J. P. 1985, Proc. Intern. Workshop on Data Analysis in Astronomy, eds. L. Scarsi and V. di Gesù (London: Plenum), p. 271
- Aoki, K., Ohtani, H., Yoshida, M., & Kosugi, G. 1996, AJ, 111, 140
- Arribas, S., Mediavilla, E., del Burgo, C., & Garcia-Lorenzo, B. 1997, in *Emission lines in Active Galaxies: New Methods and Techniques*, eds. B. M. Peterson, F.-Z. Cheng and A. S. Wilson, ASP Conf. Series, 113, 339
- Bahcall, J. N., & Ekers, R. D. 1969, ApJ, 157, 1055
- Baum, S. A., O’Dea, C. P., Dallacasa, D., de Bruyn, A. G., & Pedlar, A. 1993, ApJ, 419, 553
- Bergeron, J., Durret, F., & Boksenberg, A. 1983, A&A, 127, 322
- Bertola, F., Pizzella, A., Persic, M., & Salucci, P. 1993, ApJ, 416, L45
- Bicknell, G. V. 1995, ApJS, 101, 29
- Bicknell, G. V., Dopita, M. A., Tsvetanov, Z. I. & Sutherland, R. S. 1998, ApJ, 495, in press
- Brinks, E., & Mundell, C. G. 1996 in *The Minnesota Lectures on Extragalactic Neutral Hydrogen*, ed. E. D. Skillman, ASP Conf. Series, 106, 268
- Caldwell, N., & Phillips, M. M. 1981, ApJ, 244, 447
- Capetti, A., Macchetto, F., Axon, D. J., Sparks, W. B., & Boksenberg, A. 1995, ApJ, 448, 600
- Capetti, A., Macchetto, F., Axon, D. J., Sparks, W. B., & Boksenberg, A. 1996, ApJ, 469, 554
- Capetti, A., Axon, D. J. & Macchetto, F., 1997, ApJ, in press
- Colina, L., Sparks, W. B., & Macchetto, F. 1991, ApJ, 370, 102 (CSM91)
- Conway, J. E., & Blanco, P. R. 1995, ApJ, 449, L131
- Danziger, J. I., Goss, W. M., & Wellington, K. J. 1981, MNRAS, 196, 845 (DGW81)
- Dwarakanath, K. S., Owen, F. N., & van Gorkom, J. H. 1995, ApJ, 442, L1
- Dopita, M. A., & Sutherland, R. S. 1995, ApJ, 455, 468
- Dopita, M. A., & Sutherland, R. S. 1996, ApJS, 102, 161

- Gallimore, J. F., Baum, S. A., O’Dea, C. P., Brinks, E., & Pedlar, A. 1994, *ApJ*, 422, L13
- Grenshaw, D. M. 1997, in *Emission lines in Active Galaxies: New Methods and Techniques*, eds. B. M. Peterson, F.-Z. Cheng and A. S. Wilson, ASP Conf. Series, 113, 240
- Haniff, C. A., Wilson, A. S., & Ward, M. J. 1988, *ApJ*, 334, 104
- Heckman, T. M., Blitz, L., Wilson, A., Armus, L., & Miley, G. 1989, *ApJ*, 342, 735
- Heisler, C. A., & Vader, J. P. 1995, *AJ*, 110, 87
- Hough, J. H., Brindle, C., Axon, D. J., Bailey, J., & Sparks, W. B. 1987, *MNRAS*, 224, 1013
- Inglis, M. D., Brindle, C., Hough, J. H., Young, S., Axon, D. J., Bailey, J. A., & Ward, M. J. 1993, *MNRAS*, 263, 895
- Kotany, C. G., & Ekers, R. D. 1979, *A&A*, 73, L1
- Koyama, K., Awaki, H., Iwasawa, K., & Ward, M. J. 1992, *ApJ*, 399, L129
- Kriss, G. A., et al. 1992, *ApJ*, 392, 485
- Kriss, G. A., Espey, B. R., Krolik, J. H., Tsvetanov, Z., Zheng, W., & Davidsen, A. F. 1996, *ApJ*, 467, 622
- Jaffe, W., & McNamara, B. 1994, *ApJ*, 434, 110
- Jones, P. A., & McAdam, W. B. 1992, *ApJS*, 80, 137
- Möllenhoff, C., Hummel, E., & Bender, R. 1992, *A&A*, 255, 35
- Mathur, S. 1994, *ApJ*, 431, L75
- Mathur, S., Elvis, M., & Wilkes, B. 1995, *ApJ*, 452, 230
- Morganti, R., Sadler, E. M., & Oosterloo, T. 1997, in *The Nature of Elliptical Galaxies*, eds. M. Arnaboldi, G. S. Da Costa & P. Saha, ASP Conf. Series, in press
- Morganti, R., Sadler, E. M., Oosterloo, T., Pizzella, A., & Bertola, F. 1997, *AJ*, 113, 937
- Morse, J. A., Raymond, J. C., & Wilson, A. S. 1996, *PASP*, 108, 426
- Mulchaey, J. S., Tsvetanov, Z., Wilson, A. S., & Pérez-Fournon, I. 1992, *ApJ*, 394, 91
- Mundell, C. G., Pedlar, A., Baum, S. A., O’Dea, C. P., Gallimore, J. F., & Brinks, E. 1995, *MNRAS*, 272, 355
- Nandra, P., & Pounds, K. A. 1994, *MNRAS*, 268, 405
- Nelson, C. H., & Whittle, M. 1995, *ApJS*, 99, 67
- Pedlar, A., Dyson, J. E., & Unger, S. W. 1985, *MNRAS*, 214, 463
- Pedlar, A., Howley, P., Axon, D. J., & Unger, S. W. 1992, *MNRAS*, 259, 369
- Pogge, R. W. 1997, in *Emission Lines in Active Galaxies: New Methods and techniques*, eds. B. M. Peterson, F.-Z. Cheng and A. S. Wilson, ASP Conf. Series, 113, 378

- Prieto, M. A., & Freudling, W. 1993, ApJ, 418, 668
- Prieto, M. A., & Freudling, W. 1996, MNRAS, 279, 63
- Sault, R. J., Teuben, P. J., & Wright, M. C. H. 1995, in *Astronomical Data Analysis Software and Systems. IV.*, eds. R. Shaw, H. E. Payne and J. J. E. Hayes, ASP Conf. Series, 77, 433
- Schiminovich, D., van Gorkom, J.H., van der Hulst, J.M. & Malin, D.F. 1995, ApJ, 444, L77
- Steiman-Cameron, T. Y., Kormendy, J., & Durinsen, R. H. 1992, AJ, 104, 1339
- Taylor, D., Dyson, J. E., & Axon, D. J. 1992, MNRAS, 255, 351
- Ulvestad, J. S., & Wilson, A. S. 1984, ApJ, 285, 439
- Ulvestad, J. S., & Wilson, A. S. 1989, ApJ, 343, 659
- Unger, S. W., Pedlar, A., Axon, D. J., Whittle, M., Meurs, E. J. A., & Ward, M. J. 1987, MNRAS, 228, 671
- van Dokkum, P.G. & Franx, M. 1995, AJ, 110, 2027
- van Gorkom, J. H., Knapp, G. R., Ekers, R. D., Ekers, D. D., Laing, R. A., & Polk, K. S. 1989, AJ, 97, 708
- van Gorkom, J. H., van der Hulst, J. M., Haschick, A. D., & Tubbs, A. D. 1990, AJ, 99, 1781
- van Gorkom, J. H., Knapp, G. R., Raimond, E., Faber, S. M., & Gallagher, J. S. 1986, AJ, 91, 791
- Wagner, S. J., & Appenzeller, I. 1989, A&A, 225, L13
- Wardle, M., & Knapp, G. R. 1986, AJ, 91, 23
- Whittle M., Pedlar A., Meurs E.J.A., Unger S.W. & Ward W.J., 1988, ApJ, 326, 125
- Whittle M. 1989, in *Extranuclear Activity in Galaxies* eds. E.J.A. Meurs and R.A.E. Fosbury, ESO Conf Proc. No.32, 199
- Wilson, A. S., & Ulvestad, J. S. 1983, ApJ, 275, 8
- Wilson, A. S. 1991, in *The interpretation of Modern Synthesis Observations of Spiral Galaxies*, eds. N. Duric and P. C. Crane, ASP Conf. Series, 18, 227
- Wilson, A. S., & Tsvetanov, Z. I. 1994, AJ, 107, 1227
- Wilson, A. S., 1997, in *Emission lines in Active Galaxies: New Methods and Techniques*, eds. B. M. Peterson, F.-Z. Cheng and A. S. Wilson, ASP Conf. Series, 113, 264
- Wiklind, T., Combes, F., & Henkel, C. 1995, A&A, 297, 643

FIGURE CAPTIONS

Fig. 1.— The ATCA 8 GHz radio continuum image. The contour levels are 0.75, 1.5, 3, 6, 12, 24, 48, 96% of the peak value of $163 \text{ mJy beam}^{-1}$. Positions of the 21 cm continuum peak and of the H I absorption are marked with crosses with sizes representing the 1σ error bar.

Fig. 2.— The ATCA 1.4 GHz radio continuum image superimposed onto the DSS image. The contour levels are $2.5 \text{ mJy beam}^{-1}$ to 1.16 Jy in steps of factor 1.5.

Fig. 3.— The [O III] $\lambda 5007$ image (contours) superimposed onto the 8 GHz map (greyscale) with an enlargement of the central region.

Fig. 4.— Position-velocity slice taken along the major axis (P.A. = 120°). Contour levels: -1 to $-16.16 \text{ mJy beam}^{-1}$ in steps of $1.6 \text{ mJy beam}^{-1}$ (dashed lines) and 1 to 5 mJy beam^{-1} in steps of 1 mJy beam^{-1} (solid lines).

Fig. 5.— The H I absorption profile.

Fig. 6.— The global H I profile.

Fig. 7.— Images from the individual velocity channels (plotted every second channel). The contour levels are: $-15, -8, -4, -2, -1, 1, 1.5, 2, 3, 4, 5, 6, 7, 8, 9, 10 \text{ mJy beam}^{-1}$.

Fig. 8.— Total H I intensity map of IC 5063 superimposed onto the optical image of the galaxy. The “hole” in the center of the H I distribution (and coincident with the center of the galaxy) represents the region of strong absorption against the radio continuum. Contour levels: 1.0×10^{20} to 1.72×10^{21} in steps of 1.8×10^{20} atoms cm^{-1} .

Fig. 9.— Total H I intensity map of IC 5063 (contours as in Fig. 8) superimposed onto the [O III] $\lambda 5007$ image.

Fig. 10.— The H I velocity field of IC 5063. Contour levels range from 3100 to 3700 in steps of 20 km s^{-1} .

Fig. 11.— The distribution of the high-excitation ionized gas as outlined by the [O III] $\lambda 5007/\text{H}\alpha + [\text{N II}]$ ratio map (white contours) superposed onto the *HST* image. The enlargement shows the 8 GHz map (green contours) and the morphology of the central part of the *HST* image. The 8 GHz contours are drawn at 0.5, 1, 2, 4, 8, 16, 32, 64 % of the peak value of $163 \text{ mJy beam}^{-1}$.

TABLE 1. Properties of IC 5063

v_{helio} (km s ⁻¹) ^a	3404
Distance (Mpc) ^b	68
scale (kpc arcsec ⁻¹)	0.32
L_B (L_{\odot}) ^c	4.7×10^{10}
M_{H_2} (M_{\odot}) ^d	6.7×10^8
M_{HI} (M_{\odot}) ^e	1.0×10^{10}
M_{HI} (M_{\odot}) ^a	8.4×10^9
L_{FIR} (L_{\odot}) ^d	4.7×10^{10}
$S_{60\mu\text{m}}$ (Jy) ^f	6.53
$S_{100\mu\text{m}}$ (Jy) ^f	3.92
$S_{1.4\text{GHz}}$ (Jy) ^a	1.26
$P_{1.4\text{GHz}}$ (W Hz ⁻¹)	6.3×10^{23}

References — (a) this work; (b) assuming $H_0 = 50 \text{ km s}^{-1} \text{ Mpc}^{-1}$; (c) RC3; (d) Wiklind et al. (1995); (e) DGW81; (f) Knapp et al. (1989)

TABLE 2. H I Observations

Date	ATCA Configuration	Min-Max Baseline (m)	Bandwidth (MHz) /channels	Frequency (MHz)	Time (h)
1995 Sep	750D	31–719(4469)*	16/256	1406	12
1995 Dec	6C	153–6000	16/256	1406	5
1996 Apr	6A	337–5939	16/512	1406	12
1996 May	1.5D	107–1439(4439)*	16/512	1406	12
1996 Jun	6D	77–5878	16/512	1406	12

* the longest baseline length using also the 6 km antenna is given in parenthesis.

TABLE 3. Instrumental Parameters of the H I Observations

Field Center (J2000.0)	$20^{\text{h}}52^{\text{m}}02^{\text{s}}.0 \quad -57^{\circ}04'09''$
Synthesized beam (natural weighting)	$18''.2 \times 16''.6$, P.A. = -39.7°
Synthesized beam (uniform weighting)	$8''.2 \times 6''.7$, P.A. = -69°
Velocity of the band center (km s ⁻¹)	3290
Velocity resolution (km s ⁻¹)	26
rms noise in channel maps (mJy beam ⁻¹)	0.53